Probing cosmic ray composition with inclined air showers observed by LHAASO-KM2A

Xishui Tian,[a,*] Quanbu Gou,[b] Zhuo Li,[a,c] Giuseppe Di Sciascio,[d] Sujie Lin,[e] Mingming Kang,[f] Jinsheng Gou[g] and Qinyuan Zhang[a] for the LHAASO Collaboration

[a] *Department of Astronomy, School of Physics, Peking University, Beijing, China*
[b] *Key Laboratory of Particle Astrophysics, Institute of High Energy Physics, Chinese Academy of Sciences, Beijing, China*
[c] *Kavli Institute for Astronomy and Astrophysics, Peking University, Beijing, China*
[d] *INFN - Roma Tor Vergata, Via della Ricerca Scientifica 1, Rome, Italy*
[e] *School of Physics and Astronomy, Sun Yat-sen University, Zhuhai, Guangdong, China*
[f] *College of Physics, Sichuan University, Chengdu, Sichuan, China*
[g] *College of Materials Science and Technology, Beijing Forestry University, Beijing, China*

E-mail: tianxs@stu.pku.edu.cn

The origin of cosmic ray (CR) spectral knee around ~4 PeV is unknown. Composition studies around the knee can provide information on the CR sources and propagation. LHAASO-KM2A is capable of simultaneously measuring the EM and muonic components in extensive air showers. The triggered events of LHAASO-KM2A are dominated by CRs of higher energies at larger zenith angles because of the increasing atmospheric attenuation. In this work, we use the KM2A observed spectrum of muon-to-electron number ratio to constrain CR composition around the knee. The muon-to-electron number ratio spectra are compared between Monte Carlo (MC) simulation and experiment data over a wide zenith angle range. We report a MC excess at large zenith angles, which sets an upper limit on CR Fe flux at PeVs. Systematic uncertainties of interaction models and atmospheric models are briefly discussed.

38th International Cosmic Ray Conference (ICRC2023)
26 July - 3 August, 2023
Nagoya, Japan

*Speaker

https://pos.sissa.it/

PoS(ICRC2023)297

1. Introduction

The origin and propagation of cosmic ray (CR) are far from understood after its discovery more than a century ago. The CR energy spectrum shows power laws in general. A spectral steepening appears around 4 PeV, which marks the so-called CR spectral knee. The reason of the CR knee is unclear. Possible causes include acceleration limit of the Galactic CR sources, i.e., the maximum energy of CR that the sources can produce, and the propagation effects, i.e., the more rapid leakage of CRs from the Galaxy with increasing energy[1]. Composition observations play a key role in deciphering the physical processes accounting for the steepening in the energy spectrum. Previous experimental efforts include KASCADE[2], IceTop and IceCube[3], ARGO-YBJ and WFCT[4], and so on. However, differences between various experiments prevent a observational consensus on the CR composition around the knee.

Large High Altitude Air Shower Observatory (LHAASO)[5] is a multi-component experiment with three sub-arrays: Water Cherenkov Detector Array (WCDA), Wide Field-of-view Cherenkov Telescope Array (WFCTA) and Square Kilometer Array (KM2A). KM2A is composed of 5216 electromagnetic detectors (EDs) and 1188 muon detectors (MDs), deployed into a circle of 635 m radius. The large coverage and high altitude of KM2A make it capable of observing showers from large zenith angles. Meanwhile, independent measurements on electromagnetic (EM) component and muon component in the air showers provide reliable differentiation between mass groups.

In this work, we show the spectra of muon-to-electron number ratio of CR events at different zenith angles for the observation data and the simulation of the H3a[6] composition model. The observed spectrum at large zenith angles leads to an upper limit on Fe flux at PeV range.

2. Data and simulation

2.1 Experimental data

The data used in this analysis is from January 22, 2022 to January 31, 2022, under the steady operation of full KM2A. The triggered events are filtered by setting the minimum numbers of secondary EM and muon particles collected by EDs and MDs and that the distance of reconstructed shower core should be greater than 65 m from the array edge. Besides the event selection conditions mentioned above, the fraction of properly working detectors is greater than 99% for both EDs and MDs.

2.2 Monte Carlo Simulation

Simulated events are generated with CORSIKA 7.7410 [7] and G4KM2A.The hadronic model is QGSJet-II-04 at high energy and FLUKA at low energy. The atmosphere model used in simulation is the US standard atmosphere, with a vertical depth around 597 g cm^{-2} at LHAASO altitude. The simulated events are reconstructed and selected with the same procedure that is applied to data. The simulated shower library includes five mass groups commonly used in ground-based experiments: Proton, Helium, Nitrogen (for CNO group), Aluminum (for MgAlSi group), and Fe.

The simulated shower covers a wide range of primary energy and zenith angle: 10 TeV-100 PeV in energy, 0-89 degree in zenith angle. We use stratified sampling to simulate showers of such a wide range, i.e., the sampling is divided into small energy and zenith angle bins. For the shower energy, the simulation is linearly divided in log space with a bin width of $\Delta \log E = 1$ and the input spectrum within each bin is E^{-2}. For the zenith angle, the simulation is binned according to the increase of slant depth towards large zenith angles from 0 to 89 degree. Special options of CORSIKA are selected for simulating showers of high energy and/or large zenith angles. *THINNING* is used for secondary EM particles ($E_{\rm th}^{\rm em} = 10$ MeV) if the primary energy is higher than 1 PeV. *CURVED* is chosen for showers above 70 degree.

3. $N_\mu/N_{\rm e}$ spectra at different zenith angles

The muon-to-electron number ratio is related to the primary mass. Heavy nuclei have a larger muonic component and smaller EM component compared to light nuclei of the same energy. Therefore, heavy nuclei have larger muon-to-electron ratio than light ones. Theoretically, the spectrum of muon-to-electron number ratio encapsulates the composition information of primary cosmic rays.

Observationally, we use the number of photoelectrons (pe) collected in MDs (EDs) as the proxy of number of muons (EM particles) to study the composition evolution of cosmic rays. Hereinafter, N_μ is defined as the total number of pe in all MDs within 40-200 m,[1] from the shower axis in the shower plane. Likewise, N_e is the total number of pe in all EDs within 0-200 m from the shower axis.

3.1 Comparison between data and simulation

We compare in Figure 1 the $N_\mu/N_{\rm e}$ spectra in reconstructed zenith angle bins, $\theta_{\rm Rec}$, between data and simulation with the H3a model. Top panel shows the event rate spectra of $N_\mu/N_{\rm e}$ for data (solid line) and simulation (dashed lines), where the spectra have been vertically shifted according to the zenith angle to line up the spectra in the order of increasing zenith angles from top to bottom for better visibility. Bottom panel is the ratio between simulation and data to show the deviations of simulation at different zenith angles. An overall agreement is shown between the experimental data and the simulation in a wide range of zenith angles. Furthermore, the agreement shows that the H3a model can describe the data within 30% below 52 deg.

However, the significant discrepancy of simulation and data is the simulation excess (over 100%) around $N_\mu/N_{\rm e} \approx 2$ at zenith angle $55 - 66$ deg. This implies that the H3a model likely overestimates the flux of PeV Fe (see below).

3.2 Upper limit on CR Fe flux at PeV

The measured $N_\mu/N_{\rm e}$ spectra allow one to set upper limits on the flux of individual mass groups by requiring the simulation of any individual nucleus not overshooting the observed spectrum. Motivated by the H3a excess of $N_\mu/N_{\rm e}$ at large zenith angles, we derive an upper limit of PeV Fe flux based on the observed $N_\mu/N_{\rm e}$ spectrum at 58-66 degree.

Figure 2 zooms in on the $N_\mu/N_{\rm e}$ spectrum at $58-66$ degree by displaying the simulated spectra of different mass groups. The significant MC excess around $N_\mu/N_{\rm e} \approx 2$ is mostly contributed by Fe (shown by the cyan lines). The ratio between the spectrum of Fe and the data peaks at the same

[1] The central region is excluded for muon counting to alleviate punch-through effect of energetic EM particles near the shower axis.

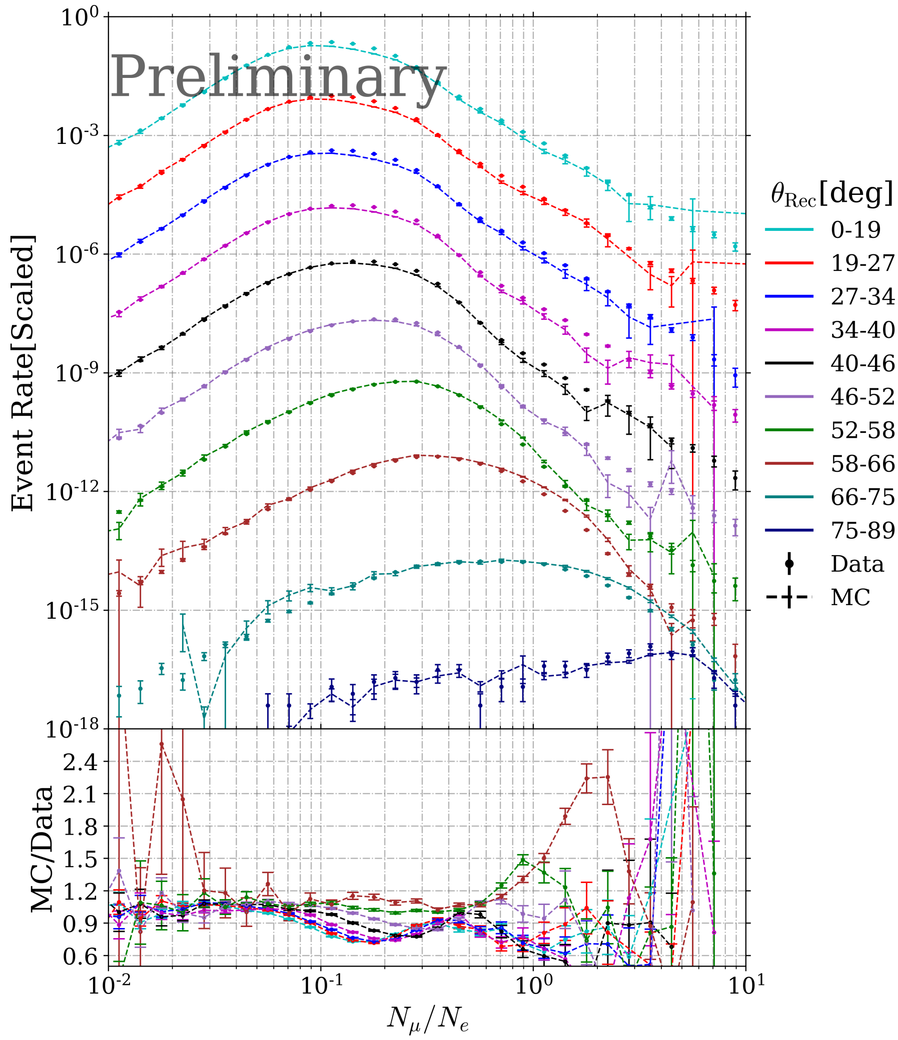

Figure 1: N_μ/N_e spectra of CR events at different zenith angles. Top panel: Comparison in different zenith angle bins between data (dots) and simulation (dashed lines) assuming H3a model. The color codes refer to different reconstructed zenith angles, θ_Rec. The y-axis has been vertically shifted for visualization. Bottom panel: The event rate ratio between simulation and data at different zenith angles. Only statistical uncertainties of simulation and data are shown. (The ratios above 66 degree are left out in the bottom panel due to poor statistics).

region. Therefore, the simulation excess at large zenith angles is most likely because the H3a model overestimates the Fe flux.

The energy spectrum of triggered events in a certain zenith angle bin usually show a sharp cutoff at low energy because of the atmospheric absorption of low energy showers, as shown in Fig 3. Because the atmospheric thickness increases at large zenith angles, the spectral cutoff energy also increases with zenith angles. At the zenith angle bin of 58-66 degree, the event rate of Fe is dominated by showers around 1.2 PeV. Therefore, the N_μ/N_e spectrum of Fe at 58-66 degree is mostly determined by PeV events.

Let us consider the upper limit on the Fe flux at PeV range, since the H3a excess at zenith angles

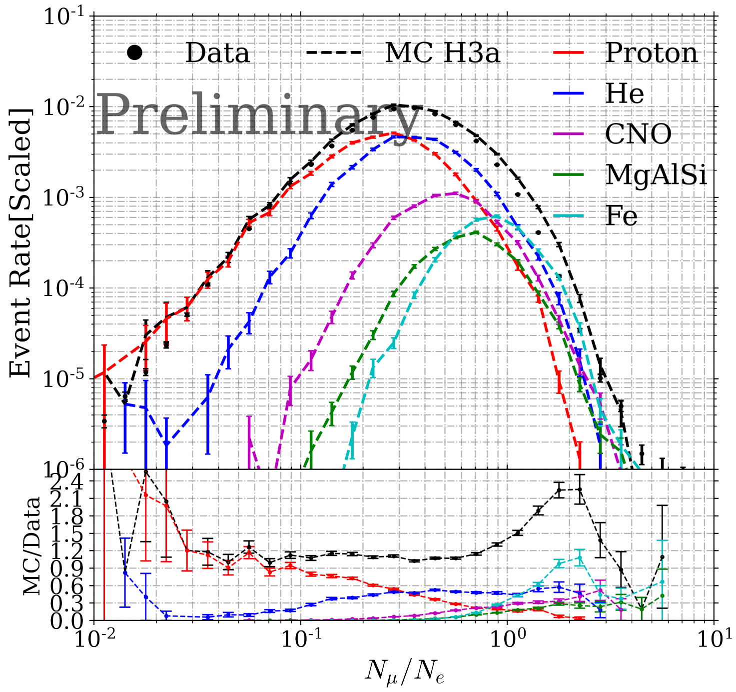

Figure 2: N_μ/N_e spectrum of CR at zenith angles of 58-66 degree. The black dashed line is simulation with the H3a model summing up all mass groups and the colorful dashed lines are results of individual mass groups given by H3a model. The colors represent different mass groups which is annotated in the figure legend. Top panel: The black dots are observed N_μ/N_e spectrum. The dashed lines are the simulation with the H3a model. Bottom panel: event rate ratio between simulation and data.

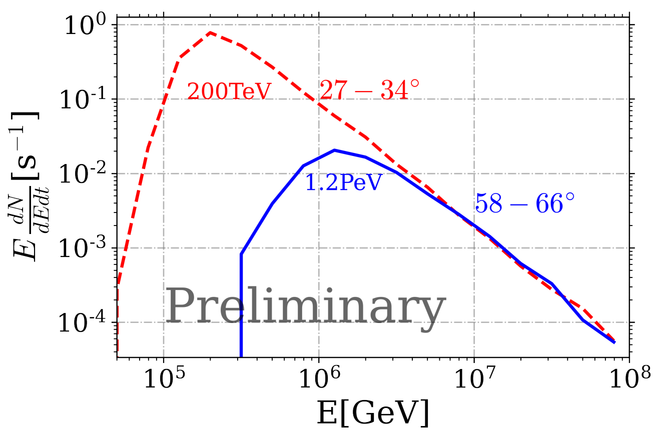

Figure 3: Simulated event rate of triggered Fe events as function of CR energy, assuming the primary spectrum is H3a model. The red dashed line is for zenith angles of 27-34 degree, and the blue solid line for 58-66 degree. The peak energy of the two angle bins are 200 TeV and 1.2 PeV, respectively.

of 58-66 degree at $N_\mu/N_e \approx 2$ is mostly determined by the flux of PeV Fe. Assuming an isotropic incidence and a CR spectrum with a flux of F_0, if the simulation of pure Fe results in an event rate of N_0 in the concerned region, i.e., zenith angles of 58-66 degree and $N_\mu/N_e \approx 2$, then the Fe flux is limited to $F_{\text{Fe}} \leq (N_{\text{Data}}/N_0)F_0$, where N_{Data} is the observed event rate.

4. Discussion

The simulation excess observed at large zenith angles shown in Fig 1 probably points to the overestimation of H3a model for heavy nuclei, i.e. Fe, around PeV. The inconsistency between data and simulation on the $N_\mu/N_{\rm e}$ spectra at large zenith angles suggests the cosmic ray composition may be lighter than the H3a model in the PeV energy range. On the other hand, we note the systematic uncertainties from atmosphere model and hadronic model are the caveat for any conclusive judgement on the CR composition

The uncertainty of atmosphere is from the daily variation of experiment conditions. The experiment data used in this analysis is from a short time window (10 days), which makes the seasonal variation of atmosphere negligible. The averaged vertical depth during the data taking period at LHAASO site is $\sim$ 599 g cm^{-2} [2] and the daily variation is roughly 1 g cm^{-2}. The vertical depth of US standard atmosphere at LHAASO altitude is $\sim$ 597 g cm^{-2}. To quantify the effects of changing atmosphere on the upper limit of PeV Fe, we repeat the analysis with a modified atmosphere model in simulation whose vertical depth is 603 g cm^{-2} (denoted as Atm603), 1% thicker than US standard model. Figure 4a compares the N_μ/N_e spectra under the two atmosphere models, Atm603 and US standard atmosphere. The bottom panels shows the ratio between the two atmosphere models. In the region of interest ($N_\mu/N_e \approx 2$), the N_μ/N_e spectrum of Atm603 is slightly smaller than that of the US standard model by less than 10%. Thus, the effects of the daily changing atmosphere on the ratio spectrum is within 10% around $N_\mu/N_e \approx 2$.

The interaction model is the major uncertainty for this analysis. We use two interaction models, Sibyll-2.3d and QGSJET-II-04, to bracket the variation induced by the imperfect hadronic modelling. Figure 4b compares $N_\mu/N_{\rm e}$ spectra of the two models. Statistically, Sibyll-2.3d predicts a smaller $N_\mu/N_{\rm e}$ than QGSJET-II-04. The ratio between Sibyll and QGSJET is approximately 0.65 around $N_\mu/N_{\rm e} \approx 2$. Therefore, the $N_\mu/N_{\rm e}$ spectrum is sensitive to the hadronic model, which is the most uncertain for this analysis.

5. Summary

We have compared the $N_\mu/N_{\rm e}$ spectra of data and simulation in a wide zenith angle range. The general agreement between data and simulation demonstrates the capability of LHAASO-KM2A observing inclined air showers and the proper treatments of simulation programs at large zenith angles.

The simulation excess at large zenith angles suggests the H3a model overestimates PeV Fe, though the uncertainties from hadronic models is large. We set an upper limit of PeV Fe, by requiring the pure Fe simulation not exceeding the observation data. The systematic uncertainties are mainly

[2]The depth is approximately calculated from the air pressure at LHAASO site, vertical depth[g cm^{-2}] $\approx 1.02P$, where P is the air pressure measured in hPa.

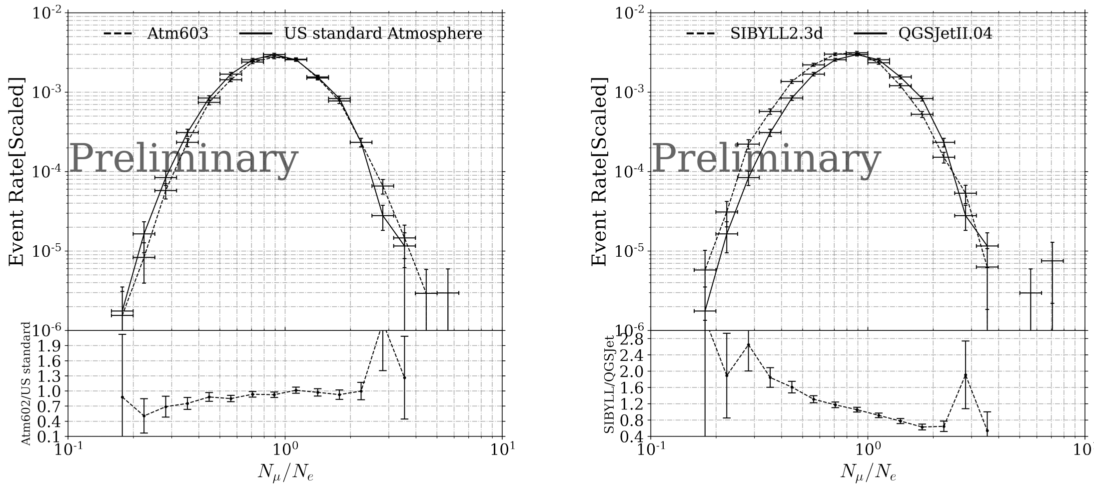

(a) **(b)**

Figure 4: Systematic uncertainties of N_μ/N_e at 58 − 66 degree for 1 − 10PeV Fe assuming $E^{-2.7}$ energy spectrum. (a) Systematic uncertainties from atmosphere models. (b) Systematic uncertainties from interaction models.

contributed by the hadronic model compared to the atmosphere model. The GST model is in tension with the observation data at large zenith angles, while the judgement of H3a model depends on the selected hadronic model. For the QGSJET model, H3a overshoots the observed spectrum at N_μ/N_e at large zenith angles. In contrast, the H3a model is more compatible with the data for the Sibyll model. Therefore, a decisive conclusion on the CR composition is largely impeded by the hadronic modelling, which calls for further investigation.

Acknowledgement

The authors would like to thank all staff members who work at the LHAASO site above 4400 meter above the sea level year round to maintain the detector and keep the water recycling system, electricity power supply and other components of the experiment operating smoothly. We are grateful to Chengdu Management Committee of Tianfu New Area for the constant financial support for research with LHAASO data. This analysis is also supported by the Natural Science Foundation of China No. U1931201, National Key R&D Program of China No.2023YFE0102300, and PIFI program of the Chinese Academy of Sciences No.113111WGZJTPYJY20200004.

References

[1] Jörg R. Hörandel. On the knee in the energy spectrum of cosmic rays. *Astroparticle Physics*, 19:193–220, 2003.

[2] T. Antoni and W. D. Apel and A. F. Badea and K. Bekk and A. Bercuci, et al. KASCADE measurements of energy spectra for elemental groups of cosmic rays: Results and open problems. *Astroparticle Physics*, 24(1):1–25, 2005.

[3] IceCube Collaboration. Cosmic ray spectrum and composition from PeV to EeV using 3 years of data from IceTop and IceCube. *Physical Review D*, 100:082002, 2019.

[4] B. Bartoli and P. Bernardini and X. J. Bi and Z. Cao and S. Catalanotti, et al. Knee of the cosmic hydrogen and helium spectrum below 1 PeV measured by ARGO-YBJ and a Cherenkov telescope of LHAASO. *Physical Review D*, 92:092005, 2015.

[5] Xin-Hua Ma, Yu-Jiang Bi, Zhen Cao, Ming-Jun Chen, Song-Zhan Chen, Yao-Dong Cheng, Guang-Hua Gong, Min-Hao Gu, Hui-Hai He, Chao Hou, Wen-Hao Huang, Xing-Tao Huang, Cheng Liu, Oleg Shchegolev, Xiang-Dong Sheng, Yuri Stenkin, Chao-Yong Wu, Han-Rong Wu, Sha Wu, Gang Xiao, Zhi-Guo Yao, Shou-Shan Zhang, Yi Zhang, and Xiong Zuo. Chapter 1 LHAASO Instruments and Detector technology. *Chinese Physics C*, 46(3):030001, March 2022.

[6] Thomas K. Gaisser. Spectrum of cosmic-ray nucleons, kaon production, and the atmospheric muon charge ratio. *Astroparticle Physics*, 35(12):801–806, 2012.

[7] D. Heck, J. Knapp, J. N. Capdevielle, G. Schatz, and T. Thouw. *CORSIKA: a Monte Carlo code to simulate extensive air showers*. 1998.